



ISSN : 2350-0743

www.ijramr.com



International Journal of Recent Advances in Multidisciplinary Research

Vol. 06, Issue 09, pp.5217-5225, September, 2019

RESEARCH ARTICLE

INHIBITION EFFECT OF ACALYPHA WILKESIANA LEAF EXTRACT ON PITTING CORROSION OF FERRITIC STAINLESS STEEL IN ACIDIC MEDIUM

*Onyinyechi Pauline Elenwo, Israel O, Owate and Michael C, Onyeaju

Department of Physics, University of Port Harcourt P.M.B.5323 Choba River State

ARTICLE INFO

Article History:

Received 27th June, 2019

Received in revised form

29th July, 2019

Accepted 20th August, 2019

Published online 30th September, 2019

Keywords:

Inhibition, Acalypha-Wilkesiana
Pitting-Corrosion; Ferritic-Stainless Steel,
Acidic Medium.

ABSTRACT

The study examined the possibility of using extract of *Acalypha wilkesiana* (AW) leaf as green inhibitor for ferritic stainless steel (FSS). This was obtained in 0.5 M hydrochloric acid using gravimetric and potentiodynamic polarization (Tafel plots). The inhibitor, temperature and time concentration ranged from 0–10 percent v / v at 2 percent v / v interval to 30–60 ° C at 10 ° C interval at 3-18 days within a space of three days. Qualitative and quantitative analysis and Fourier Transforms Infrared (FTIR) Spectroscopy technique were used to characterize the sample. Scanning electron microscope (SEM) was used to analyze the sample surface morphology before, during and after testing. The findings showed that the corrosion rate increased with an rise in temperature and decreased with an rise in inhibitor concentration and time and acquired a peak inhibition effectiveness of 91.16 percent at an optimum 8 percent v / v concentration. The coupon's SEM without extract on the surface was rough, serious pits, cracks, and intermetallic dissolution occurred. There was an enhancement with a soft green inhibitor on the surface morphology of ferritic stainless steel. The adsorption and physisorption in nature of the extract obeys Langmuir adsorption isotherm. The inhibition effectiveness values acquired are well above a good inhibitor's minimum acceptable threshold of 70 percent. Therefore, the *Acalypha wilkesiana* (AW) extract was very efficient in inhibiting FSS corrosion in acidic medium.

INTRODUCTION

Stainless steels are significant class of metals and are frequently considered as the primary piece of current industry. However, stainless steel is secured with an exceptionally defensive film of chromium oxy-hydroxide and is impervious to corrosion in numerous dynamic environments (Khatak and Baldey, 2002). It experiences uniform just as setting corrosion under certain uncommon conditions, for example, acid pickling, mechanical acid cleaning, acid de-scaling and oil well acidizing (Okamoto, 1973 and Sharma & Roy, 2014). Setting corrosion is a confined corrosion processes that outcome in the development of minuscule gaps in metallic composites. Corrosion zenith outline at infinitesimal sizes and underneath, as a result of defects, scratches, breakages and splits on the uninvolved film prompting pit solutions on the metal surface particularly in areas or locales of incorporations or polluting influences (Borgioli et al; 2016 and Zhang et al; 2015). These destinations become anodic while obscure, yet conceivably tremendous territory ends up cathodic. The corrosion spreads auto catalytically infiltrating the metal guilefully. Oneself enacting response systems related with setting begins at the surface in various structures and sizes relying upon the metallurgical property of the compound, the electrolyte and other electrochemical variables (Okamoto, 1973).

*Corresponding author: Onyinyechi Pauline Elenwo,
Department of Physics, University of Port Harcourt P.M.B.5323
Choba River State.

Setting is more harmful and risky than general corrosion since it is hard to find out right now and to structure against. An irrelevant little pit with minuscule metal misfortune can prompt breakdown of a framework (Kadry, 2008). Crumbling and shortcoming of the constructional material can cause difficult issues that had prompted the misfortunes of lives and gear, so it winds up basic to secure materials against corrosion in such forceful conditions (Fattah Alhossein et al; 2016). Security of these constructional materials from being consumed is not significant for expanding the life expectancy of materials, yet in addition significant in shielding our surroundings from dangers coming about because of the debacles (Szpowski, 2002). Notwithstanding, a significant methodology embraced for the insurance of this material against corrosion is by the utilization of inhibitors which is one of the various methods for relieving corrosion in any environments (Granese et al; 1992). The utilization of concoction inhibitors is regularly the most commonsense and financially savvy methods for corrosion moderation. Nonetheless, a large portion of these engineered inhibitors, for example, chromates, nitrates, borates, molybdates had demonstrated great enemy of destructive activity however profoundly lethal to both people and conditions as pointed by (Suleiman and Sani, 2017). An option must be looked to supplant the costly and poisonous blended corrosion inhibitors due to natural guidelines so as to elevate the practical greenness to the air. The issue of poisonous quality has prompted the utilization of normally happening substances so

as to discover ease and non-dangerous inhibitors. Plant concentrates have turned out to be significant as an ecologically worthy, promptly accessible and sustainable wellspring of materials for a wide scope of corrosion counteractive action details. In this way, discovering normally happening substances as corrosion inhibitors is a subject of extraordinary viable significance (Suleiman & Sani, 2017 and Al – Moubardi, et al; 2015). Concentrates of plants contain natural mixes, for example, N, O, P and S ions which are viewed as viable corrosion inhibitors. The viability of natural inhibitors, in any case, relies upon the nature and the state of the metallic surface, the concoction synthesis and structure of the inhibitor (Emran, et al; 2015). All plant items are natural in nature and their constituents, for example, tannins, natural and amino acids, saponins, alkaloids, flavonoids, glycosides and colors are known to show repressing activity (Pereira, 2012 and Al-Fakih, 2015). Previous works on the use of organic inhibitors to protect the materials in hydrochloric acid have been studied by (Suleiman and Sani 2016 and Adindu and Oguzie, 2017). Nonetheless, there is still a need for research on other organic compounds that can be used as inhibitors in industrial applications. *Acalypha wilkesiana* (copper leaf, Joseph's coat) is of the Euphorbiaceae family. The plant has antimicrobial and antifungal properties and in conventional prescription, the leaves are eaten as vegetables in the administration of hypertension, being a diuretic plant. Figure 1 shows the picture of *Acalypha wilkesiana* (AW) leaf. The goal of this work was to explore the corrosion inhibition of FSS in 0.5M HCl solution using AW extract as a novel green corrosion inhibitor by using gravitational weight loss and potentiodynamic polarization techniques, characterizations of the extract by analytical and FTIR methods and Scanning electron microscopy (SEM),

MATERIALS AND METHODS

Preparation of the substrates: The chemical compound of the stainless steel utilized for this work is being displayed on Table 1. Ferritic stainless steel coupon plates of measurement steel of rectangular shape with lengths of 12.5 mm, width of 6.5 mm, and thickness of 1.5 mm were acquired for this work. The substrates were treated by solutions operations including the accompanying: cutting, granulating and cleaning using (500–1500) emery paper, washing and drying. The substrates were likewise treated by utilizing 10% HCl to pickle them at room temperature for 10 s, and washed with refined water, flushed in ethanol, degreased with CH₃)₂CO, dried and put away in a desiccator (Suleiman and Abdulwahab, 2016 and Ahmed et al; 2014).

Solution Preparation: Solutions of 0.5 M HCl were set up in order to dilute systematic grade with twofold refined (distilled) water. Concentrate was dissolved in the acid solution at the required concentration (% v/v). The solution without inhibitor was taken as clear for correlation purposes. The test solutions were newly arranged before each trial by adding *Acalypha wilkesiana* straight to the acid solution. Concentration of *Acalypha wilkesiana* extract 0, 2, 4, 6, 8, and 10 % v/v. Examinations/tests were performed in triplicate to guarantee great outcomes.

Inhibitor Preparation: *Acalypha wilkesiana* (AW) used was obtained from the university of Port-Harcourt, Rivers State in Nigeria. The AW was extracted in 1.5 litres of 70% ethanol and 30% distilled water as solvent and half the AW was extracted

using maceration method. The ethanol was evaporated by using a water bath and the concentration of the stock solution expressed in terms of (% v/v) and the concentration of 2–10% v/v of the extract as prepared according to (Adindu and Oguzie, 2017 and Kubmarawa, et al; 2007).

Characterization of *Acalypha wilkesiana* (AW) by phytochemical and FTIR analyses: The phytochemical constituents were carried out by qualitative/quantitative methods at National Research Institute of Chemical Technology, Zaria. The qualitative and quantitative results showed that the *Acalypha wilkesiana* (AW) leaf contains Saponins, Tannins, Alkaloids, Flavonoids, Glycosides and Volatile oil. Fourier Transforms Infrared (FTIR) analysis was carried out to determine the functional groups and chemical bonds. It was carried out using -8400S spectrophotometer Shimadzu Product Japan at National Research Institute Chemical Technology Zaria. The spectra recorded and the interpretations were done by using Standard Library. Both the phytochemical analyses and FTIR were presented in tables 2 and 3 respectively.



Figure 1. *Acalypha wilkesiana* (AW) copper leaf or Joseph's coat leaf

Methods used for corrosion techniques: Previously polished and degreased stored coupons were used for weight loss studies. Specimens that have been weighed differently soaked in 500 mL of 0.5 M HCl solutions containing 0, 2, 4, 6, 8 and 10% v/v of AW extract for 3, 6, 9, 12, 15, and 18 days. After sometime, when it was time, the specimens were taken out, washed, dried and reweighed. The staged up experiments were carried out thrice while at the same time their mean values were put down. This experiment was repeated 4 times with varying temperatures of 30, 40, 50, and 60 °C, respectively. From the deliberate weight reduction information, the corrosion rate (mpy) and the restraint productivity (inhibition efficiency) (IE) were determined utilizing equipments 1 - 3 (Adindu and Oguzie, 2017). The corrosion rate (CR) of the material loss as a result of chemical reaction can be expressed as the thickness loss of the stainless steel per unit time:

$$CR = \frac{534W}{DAT} \quad 1$$

Where W is the weight loss after exposure of time t, D and A are the density and exposed area while the 534 is a constant respectively. CR in mils per year (mpy) and W, D, A and t will be in units of milligrams, grams per cubic centimeter (g/cm³), square inches and hours.

$$\left(\frac{CR_a}{CR_p}\right) \times 100 \quad 2$$

$$\theta = \frac{CR_a - CR_p}{CR_a} \quad 3$$

Where CR_a , CR_p and θ are corrosion rates in the absence, presence and degree of surface coverage of the inhibitor respectively.

Potentiodynamic Polarization (Tafel plots): All test have been completed in open circuit potential (OCP-T) under barometrical conditions at a temperature of 30°C utilizing three-cathode frameworks including a calomel reference terminal, a platinum plate as the helper anode and ferritic stainless steel tests as working anode that drenched in 0.5 M HCl solutions. In Tafel test, after a deferral of around 15 minutes, the potential was expanded with 1 mV/s filtering rate. The required information were gotten utilizing the above programming. From the exploratory estimations, the estimations of corrosion potential (E_{corr}), corrosion current thickness (I_{corr}) anodic and cathodic Tafel slope constants (ba and bc) can be assessed from the anodic and cathodic points of Tafel plots. However, the extrapolation of the linear Tafel portion of the anodic and cathodic plot to corrosion potential was done to obtain corrosion current densities (I_{corr}). The inhibition efficiency (IE %) of the inhibitor was calculated using equation 4 (Adindu and Oguzie, 2017):

$$IE \% = \frac{i_{corr} - i'_{corr}}{i_{corr}} \times 100\% \quad 4$$

where i_{corr} and i'_{corr} are the rust current densities of ferritic stainless steel in the absence and occurrence of the inhibitor respectively as described (Suleiman and Abdulwahab, 2016).

SEM investigations: The stainless-steel surface was prepared for SEM by keeping the specimens for one hour in the electrolyte, with and without the ideal fixations of the inhibitor. The treated steel examples were then washed with refined water, dried and broken down utilizing SEM. A Philips model XL30SFEG examining electron microscope was utilized for surface examination. The stainless-steel surface, as described by Suleiman et al; (2018).

RESULTS AND DISCUSSION

Chemical Composition of ferritic stainless steel: Table 1 showed the chemical composition of the as-received ferritic stainless steel which was determined by spark analysis at Federal University of Technology, Owerri, Nigeria.

Characterization of *Acalypha wilkesiana* (AW) Phytochemical analyses: The Quantitative and qualitative phytochemical screenings of the leaf extract (*Acalypha wilkesiana*, AW) in percentage (%) and mg/100mg results are presented in Tables 2 and 3. The results also indicated that the leaf extract contains tannins, alkaloids, flavonoids, saponins, glycosides and volatile oil.

Fourier Transforms Infrared (FTIR) Spectroscopic methods: Table 4 showed the peaks and intensity while table 5 showed the outstanding peak obtained from reflectance for AW extract reflectance FT-IR spectroscopy. The IR absorption bands between 524.66 to 3402.54 cm^{-1} for *Acalypha wilkesiana* indicated the presence of Sulfides compound (SxOy compounds, P=O vibration for stretching vibrator organic phosphorustion, CH_2 , R-CH=CH-R, C=CH₂ mono, 1,1, C=C stretch, -N=C=S, C≡N, CH₂, NH₂, X≡Y and X=Y=Z, NH₂ functional groups which fit well with these constituents.

Table 1. Elemental composition of ferritic stainless steel employed for the study

S.No.	Metal	(Wt. %) Elemental Composition
1	Fe	Balance
2	C	0.0880
3	Si	0.471
4	Mn	9.230
5	P	0.112
6	S	0.0294
7	Cr	17.42
8	Ni	1.15
9	Mo	<0.001
10	Cu	0.791
11	Al	0.0061
12	Ti	0.0137
13	V	0.0968
14	Co	0.129
15	Nb	0.029
16	Sn	0.0195
17	Pb	0.0208
18	Mg	0.0103
19	As	0.0887
20	Ce	0.0111
21	Ta	0.150
22	Zn	0.273
23	N	0.0414

Figures 2 and 3 presented the results of chemical bonds/functional groups of IR absorption spectrum of AW extract from the tables.

Weight loss (WL) measurements: The corrosion rate was displayed on Figure 4, as well as the time for the corrosion of ferritic stainless steel (FSS) in 0.5 M HCl containing various concentrations of AW at 30°C. From the figure, it is evident that the corrosion rate of ferritic stainless-steel decreases with increase in the concentration of AW. The corrosion rate of the FSS in the absence of the inhibitor (blank) solution was higher than those obtained for solutions of HCl containing various concentrations of AW. The viability of the concentrate is focus ward and corrosion rate then again diminishes as grouping of the concentrate increments. The decline in the corrosion rates can be ascribed to a portion of the constituents that were contained in the extract such as functional groups, hydroxyl, aromatic / heterocyclic rings compounds present and the metallic elements that reacted with some cations to form protective films on the samples. Similar trends have been reported in the study by (Al-Fakih et al; 2015 and Suleiman and Abdulwahab, 2016). Table 6 analysis on the optimum concentration for *Acalypha wilkesiana* (AW) was 8% v/v with utmost reticence competence (inhibition efficiency) of 91.16% for the period of 12 days of immersion time. This result indicated that the plant extract could act as effective corrosion inhibitor for FSS in the hydrochloric acid medium. This indicated that the reaction of the inhibitor on the surface of the FSS has reached the state of equilibrium. The decrease in corrosion was also attributed to the compounds/elements obtained from the phytochemical and FTIR results as shown above contain some hetero-atoms. The thin cover of the oxides comply to the metal surface leading to a reduction in corrosion rate thereby increasing the efficiencies and similar results had been reported by (Umoren, and Mohammed, 2016 and Suleiman 2018).

Potentiodynamic polarization: The results presented in Figure 5 demonstrated the impact of AW extract on both cathodic and anodic polarization curve of ferritic tempered steel in 0.5 M HCl. It could be seen that both the cathodic and anodic responses were stifled with the expansion of explored green inhibitor extricate, which proposed that AW concentrate decreased anodic disintegration and furthermore hindered the hydrogen advancement response.

Table 2. Quantitative analysis of *Acalypha wilkesiana* (AW) leaf

S/No	Leaf	Alkaloids (%)	Tannins (mg/100 g)	Saponins(%)	Flavonoids (%)	Glycosides (mg/100 g)	Volatile oil (%)
1	AW	10.04	1281	6.98	6.32	870	3.03

Table 3. Qualitative analysis of *Acalypha wilkesiana* (AW) leaf

S/No	Leaf	Alkaloids	Tannins	Saponins	Flavonoids	Glycosides	Volatile oil
1	AW	++	+++	++	+	+++	+

Heavily present: +++; slightly present: ++; present: +; absent: -

Table 4. Peaks and intensity for AW extract from reflectance FT-IR spectroscopy

No.	Peak	Intensity	Corr. Intensity	Base (H)	Base (L)	Area	Corr. Area
1	524.66	72.150	1.261	547.0	406.00	0.439	0.239
2	609.53	68.601	4.029	640.39	563.23	11.624	1.021
3	663.53	71.006	3.654	848.71	640.39	20.266	1.391
4	902.72	86.953	0.878	918.15	848.71	3.77	0.198
5	1041.6	80.157	7.050	1072.46	918.15	23.783	3.248
6	1149.61	55.623	11.653	1280.78	1072.46	42.042	6.074
7	1334.78	65.863	3.955	1357.93	1280.78	12.377	1.095
8	1381.08	67.031	2.511	1489.1	1357.93	19.126	1.511
9	1635.69	49.735	38.148	1851.72	1489.1	49.14	31.158
10	2353.23	65.141	22.624	2399.53	1867.16	26.252	6.966
11	2870.17	63.372	0.443	2877.89	2399.53	55.43	-5.714
12	2931.9	56.567	4.666	2985.91	2877.89	24.764	1.739
13	3402.51	23.246	1.136	3734.31	3394.83	130.488	-1.365

Table 5. Prominent peaks obtained from reflectance FTIR spectroscopy for AW extract

No.	Frequency (cm ⁻¹)	Band assignment
1	524.66	Metal -O- metal group
2	609.53	C-I Stretching of iodol compounds
3	663.53	C-Br Stretching of halogen derivatives
4	902.72	Thiocarbonyl (C=S)
5	1041.6	Sulphides compound (SxOy compounds)
6	1149.61	Symmetric stretching of amino acids
7	1334.78	P=O Vibration for stretching vibrator organic phosphorustion
8	1381.08	C(CH ₃) ₃
9	1635.69	N-H in =plane bending mainly proteins
10	2353.23	PH acids) stretches (Phosphoric
11	2870.17	CH ₂ Symmetric stretching of amino acids
12	2931.9	C-H stretching mainly lipids
13	3402.54	N-H stretching amine

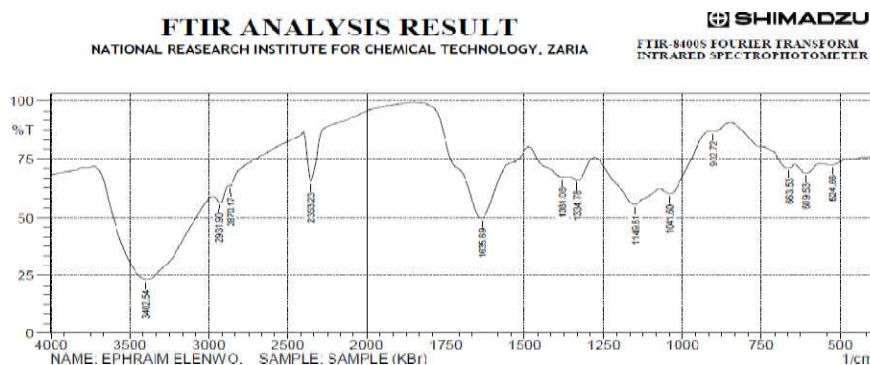


Figure 2. IR absorption spectrum of AW bark extract

Electrochemical corrosion energy parameters, for example corrosion potential (E_{corr}), cathodic and anodic Tafel slants (β_a , β_c) and corrosion current thickness (i_{corr}) got from the extrapolation of the polarization bends, were additionally given in table 7 were calculated using equation 4. The values given in the tables show that, corrosion current (i_{corr}) decreases noticeably in the occurrence of the extract. The magnitudes of change increase with increasing extract inhibitor concentrations.

This confirms the inhibitive action of the AW on ferritic stainless steel in hydrochloric. The current densities decrease with increase in the extract concentrations from 2-10% v/v, which suggests that passive layer on the surface of ferritic stainless steel is strengthened in the presence of extract due to blockage of active sites on the electrode surface and agreed to (Ahmed et al;2014 and Anupama, et al;2016). This decrease in i_{corr} was related to the adsorption of the inhibitor on ferritic stainless steel/acid solution interface and confirmed to the

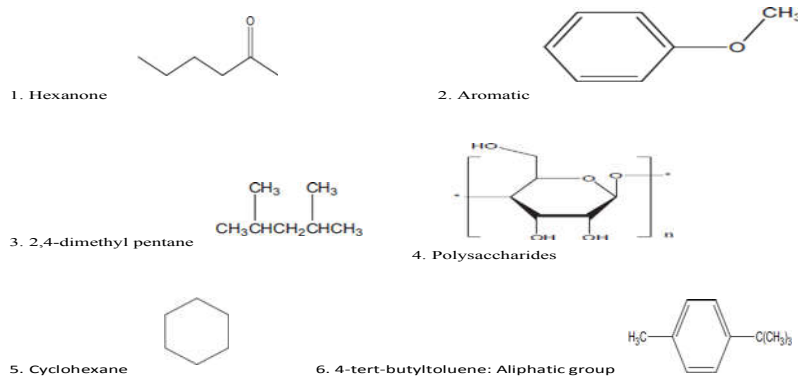


Figure 3. Chemical bonds/Functional groups of IR Absorption Spectrum of AW Extract

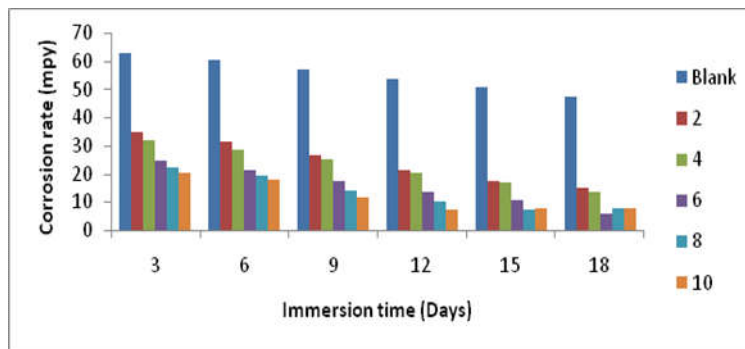


Figure 4. Variation of Corrosion rate with immersion time of AW extract for stainless steel in 0.5 M HCl solution at 30 °C

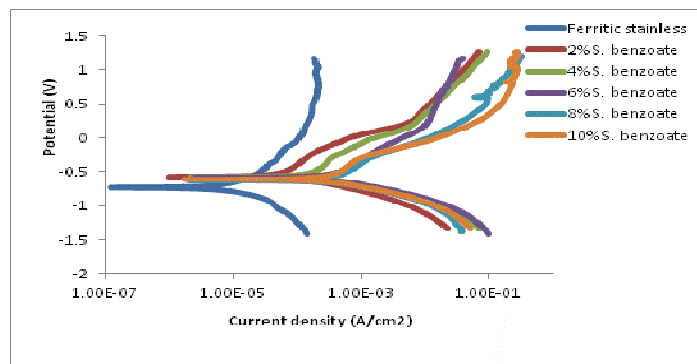


Figure 5. Potentiodynamic polarization curves for the dissolution of ferritic stainless steel in 0.5 M HCl in the absence and presence of AW extract concentrations at 30 °C

Table 7. Potentiodynamic polarization parameters for ferritic stainless steel in 0.5M HCl containing different concentrations of AW extract at 30 °C

AW (%v/v)	-E _{corr} (SCE) (mV)	i _{orr} (mA/cm ²)	Tafel slopes (mV/decade)	b _a b _c	Inhibition efficiency (IE %)
Control	0.512	9.86	62	87	-
2	0.526	3.08	65	86	68.70
4	0.528	2.76	68	88	72.00
6	0.557	1.62	65	86	83.57
8	0.529	1.25	68	85	87.32
10	0.554	0.50	73	88	92.01

Table 8. Parameters from Langmuir Isotherm for AW at 30 - 60 °C in 0.5 M HCl solution

Inhibitor	Temp. (°C)	LANGMUIR ISOTHERM			
		ΔG _{corr} , KJ/mol	Slope	R ²	K _{ads}
AW (0.5 M HCl)	30	-11.278	1.223	0.989	1.585
	40	-11.767	1.175	0.996	1.441
	50	-12.166	1.097	0.998	1.284
	60	-12.321	1.067	0.997	1.154

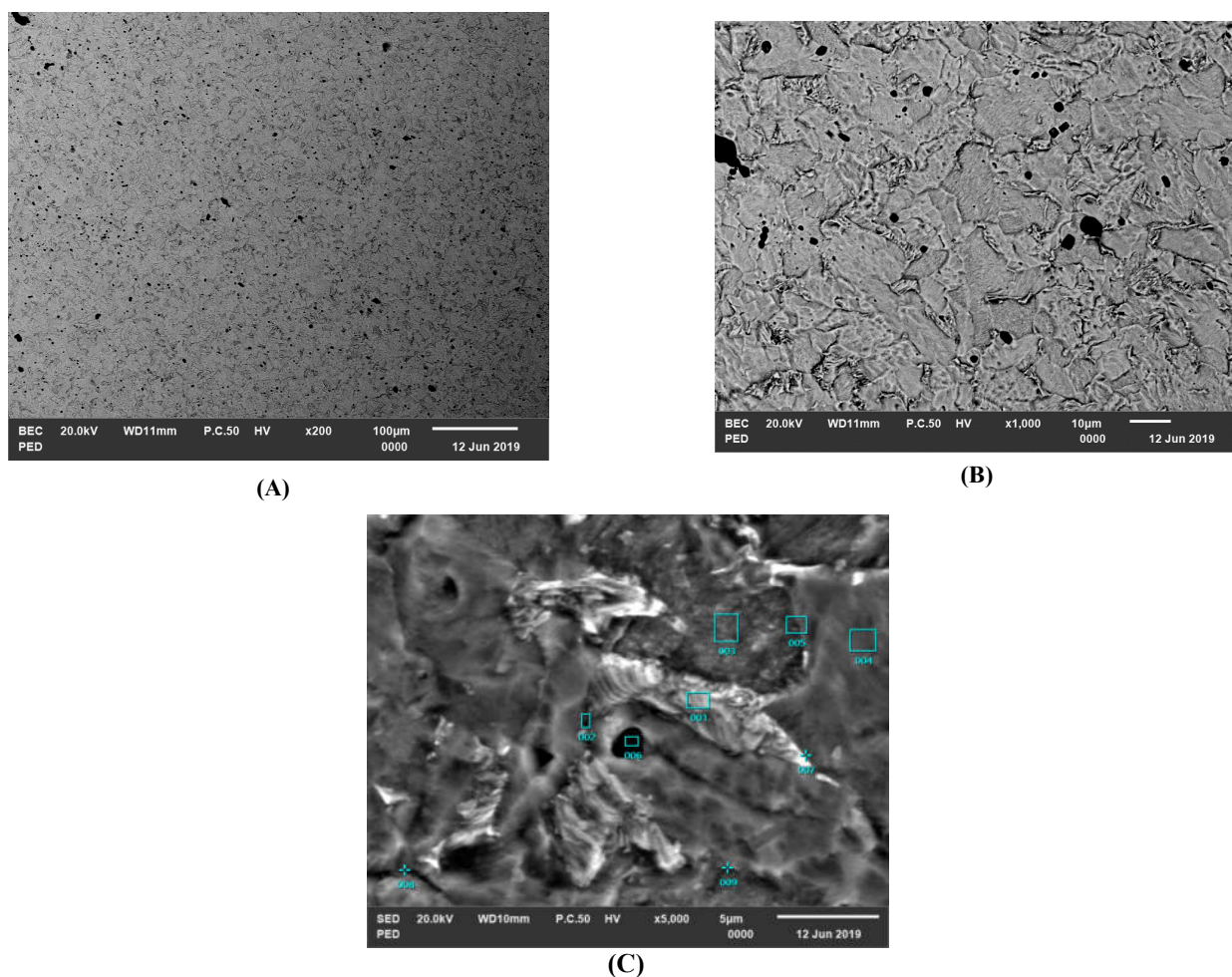


Figure 6. SEM micrographs of stainless-steel surface (a) free surface of ferritic stainless steel, (b) after immersion in 0.5 M HCl and (c) after immersion in 0.5 M HCl + 8% v/v of AW.

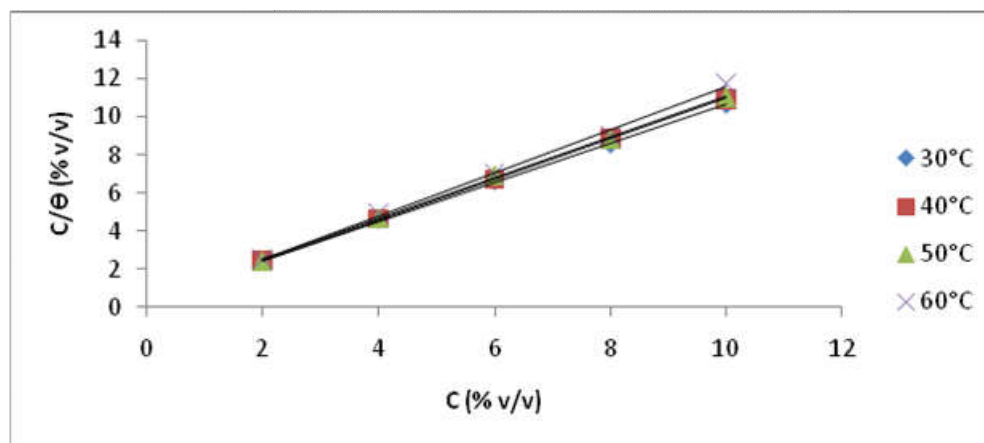


Figure 7. Langmuir adsorption isotherm as C/θ versus C of AW extract for corrosion of FSS in 0.5M HCl solution at 30, 40, 50, and 60°C

Table 9: Activation parameters E_a , ΔH_{ads} and ΔS_{ads} for FSS dissolution in 0.5M HCl in the absence and the presence of AW at 30, 40, 50, and 60°C

System/concentration	E_a (kJmol ⁻¹)	ΔH_{ads} kJ/mol	ΔS_{ads} (J/mol. k)
Blank	6.89	10.68	-19.65
2% v/v AW	8.18	11.71	-18.91
4% v/v AW	14.55	13.29	-18.62
6% v/v AW	15.24	13.84	-17.97
8% v/v AW	19.63	14.90	-17.52
10% v/v AW	21.29	15.23	-16.81

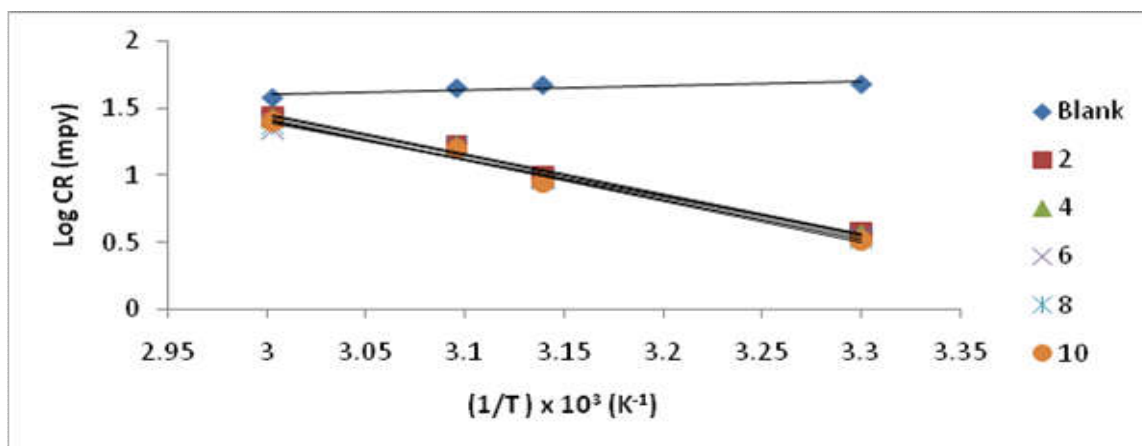


Figure 9: Variation log CR with $1/T$ for FSS in 0.5 M HCl in the presence and absence of *AW* concentration at 30, 40, 50, and 60°C

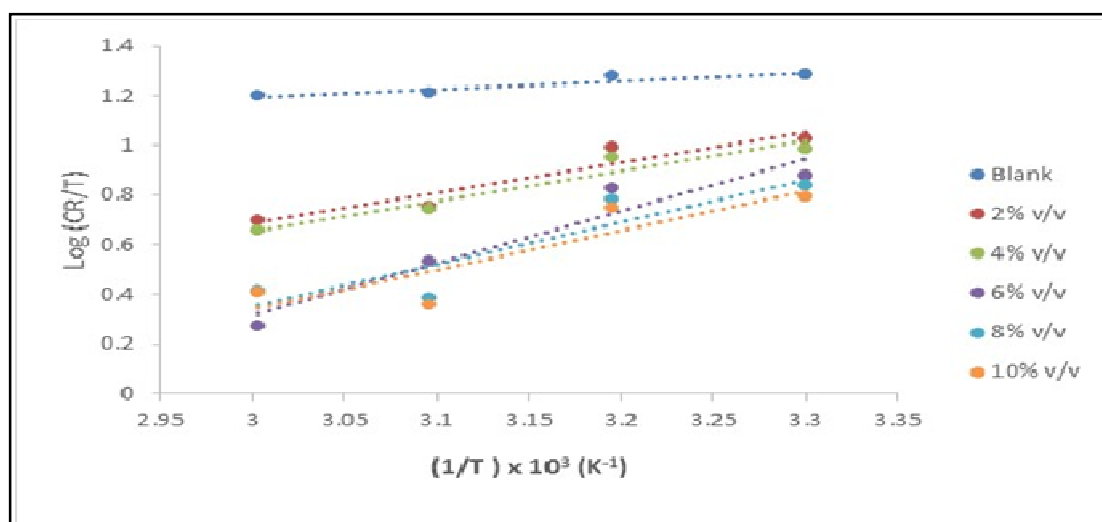


Figure 10: Variation log CR/T with $1/T$ for FSS in 0.5 M HCl in the presence and absence of *AW* concentration at 30, 40, 50, and 60°C

previous works (Suleiman and Abudlwahab, 2016 and Verma, et al.).

Surface characterization: The morphology of the examples without and with inhibitor of *Acalypha wilkesiana* (*AW*) was inspected and the outcomes exhibited in figure 6a-c. It just uncovered the cleaned/scratched surface. From the surface morphology of uninhibited FSS in 0.5 M HCl interface in figure 6b, serious pits, cracks and particular disintegration of inter-metallic happened at the surface. In figure 6c, there was an improvement in the surface morphology of FSS in the nearness of *Acalypha wilkesiana* (*AW*). From the SEM assessment, it is clear that a portion of the dynamic constituents in the phytochemical and the FTIR such as CH_2 , $\text{R}-\text{CH}=\text{CH}-\text{R}$, $\text{C}=\text{CH}_2$ mono, 1,1, $\text{C}=\text{C}$ stretch, $-\text{N}=\text{C}=\text{S}$, $\text{C}\equiv\text{N}$, CH_2 , NH_2 , $\text{X}=\text{Y}$ and $\text{XY}=\text{Z}$, NH_2 act as reaction centre leading to the formation of film on the surface of FSS (Suleiman and Sani, 2017 and Ahmed et al.; 2014). The inhibitor therefore forms a protective thin layers and complexes on the FSS surface. This leading a reduction in contact between FSS and the forceful process experienced on the inhibition effect arranged in sequence according to Suleiman et al.; (2018) and Verma et al.; (2016).

Adsorption isotherms: Adsorption isotherm gives the connection between the coverage of an interface with the adsorbed species and the concentration of species in solutions.

The utilization of adsorption isotherms gives valuable understanding into the corrosion reticence system. The estimations of the level of surface inclusion (θ) were assessed at various centralizations of the inhibitor in 0.5 M HCl solution. Efforts were formed to fit θ values to various adsorption isotherms (El-Awady, Freundlich, Frumkin, Temkin and Langmuir models) as depicted by (Szpowski, 2002 and Emran et al.; 2015): The inhibitor was found to obey Langmuir isotherm with a plot of C/θ versus C which was direct. From Figure 7, the adsorption of various groupings of *Acalypha wilkesiana* (*AW*) extract on the outside of FSS was found to obey Langmuir adsorption isotherm. The phytochemical constituents of *Acalypha wilkesiana* (*AW*) showed that these compounds were hydrolysable and can without much of a stretch be adsorbed on the metal surface by means of the solitary pair of electrons present on their oxygen particles and make a boundary for charge and mass transfer prompting decline in the collaboration of the metal with the destructive condition and thus, the corrosion rate of the metal diminished with increment in the concentrate (Pereira, 2012 and Doner, et al.; 2012). The development of film layer basically squares release of H^+ and disintegration of metal particles was then fulfilled. Acid pickling inhibitors containing natural N, S and OH^- gatherings act also to restrain corrosion (Al-fakih et al.; 2015 and Suleiman and Sani, 2016). It pursues that hindrance proficiency (IE) is legitimately corresponding to the portion of the surface secured by the adsorbed particles (θ).

Thusly, (θ) with the concentrate focus indicates the adsorption isotherm that depicts the system (Khadraoui et al; 2014). The thermodynamic parameters for the adsorption of the concentrate on FSS surface in 0.5 M HCl at various temperatures were exhibited in table 8. From the table, it was discovered that the negative estimations of ΔG°_{ads} reflect that the adsorption was unconstrained procedure and ΔG°_{ads} values increment (become more positive) with an expansion in temperature. K_{ads} diminishes as the temperature expands which likewise affirm that the green inhibitor was adsorbed and repressed the corrosion. This demonstrated the event of exothermic procedure whereby, adsorption was ominous with expanding response temperature was the aftereffect of the concentrate desorption from the FSS surface (Pereira, 2012).

Kinetics/Thermodynamics Consideration: To examine the impact of temperature on the hindrance adsorption system of *Acalypha wilkesiana* (AW) in acidic solutions in the nonattendance and nearness of fixation from 0–10% v/v, ponders were completed at various temperatures (303–333 K) by weight reduction estimations at eighteen (18) days of inundation time. It was seen that the corrosion rate increments both in the uninhibited and hindered with increment in temperature. The nearness of inhibitor prompts decline in the corrosion rate and restraint productivity additionally decline with increment in temperature, implying that the corrosion procedure is temperature dependant (Khadraoui et al; 2014 and Hong, et al; 2013). The decline might be because of increment in the pace of disintegration procedure of FSS and incomplete desorption of the inhibitor from the metal surface with increment in temperature (Ahmed, et al; 2014 and Suliema, et al; 2018) and been presented in Figure 8.

Figure 8: Variation of inhibition efficiency of extract with temperature in 0.5 M HCl solution

The corrosion rate in acidic solution is associated with Arrhenius equation of temperature provided in equation 5 (Verma et al; 2016 and Xhanai et al; 2016):

$$CR = A \exp(-E_a/RT) \quad 5$$

A weight loss assessment log of the corrosion rate versus $1/T$ showed a straight line with a path of $-E_a/2.303R$ (shown in figure 9). Table 9 also presents the activation energy values. The data show that in the presence of extract, the activation energy (E_a) of FSS corrosion is higher in 0.5 M HCl solution than in uninhibited. In this research, the rise in the evident activation energy for FSS dissolution in inhibited solution can be viewed as physical adsorption that supports our previous results from the job and comparable to the job of FSS (Umoren and Eduok, 2016) and Suleiman et al; 2018). An alternative formulation of Arrhenius equation was used to calculate the ΔH_{ads} and ΔS_{ads} in equation 6 (Suleiman et al; 2018 and Verma et al; 2016):

$$\log(CR) = -E_a/2.303RT + A \quad 6$$

The plots of $\log(CR/T)$ versus $1/T$ were shown in Figure 10 as a straight row with slope and interval equal to $-H_{ads}/2.303R$ and $(\log(R/Nh) + S_{ads}/2.303R)$ respectively from which the values of the slope and intercept had been calculated. Table 9 presented the calculated values for the green AW inhibitor in 0.5 M HCl for the activation energy, standard free energy change, E_a , ΔG°_{ads} , ΔH_{ads} , and ΔS_{ads} for the green

AW inhibitor. From the figure, the slope and intercept equals $-H_{ads}/2.303R$ and $(\log(R/Nh) + S_{ads}/2.303R)$ respectively from which the values of S_{ads} and H_{ads} were then evaluated. The values of S_{ads} and H_{ads} are positive and negative, the positive sign of H_{ads} indicates that the adsorption of the inhibitor molecules is an endothermic process, while the values of S_{ads} in the presence of AW are negative, m. The values of E_a in table 9 were greater in the presence of AW is (21,29 kJ/mol) than in the presence of uninhibited solution (6,89 kJ/mol). It has been created that the value of the activation energy ($E_a > 80$ kJ/mol means chemical adsorption while $E_a < 80$ kJ/mol implies (physical adsorption) (Qian et al; 2017 and Rubaye et al; 2015). Consequently, the rise in the activation energy can be viewed as physical adsorption that still satisfies previous claims. (Rocha et al; 2014 and Deyab, 2015).

Conclusion

The following conclusions can be drawn from the study investigated:

- The isothermic adsorption of Langmuir corresponds to the experimental data acquired in this research. Thus, on the ferritic stainless steel surface, a monolayer film was formed by the extract and the values of E_a , G_{ads} , H_{ads} and S_{ads} obtained proposed physical adsorption phenomena for inhibitor adsorption.
- The mechanism engaged in this research was the phytoconstituents of the green powder that was adsorbed on the surface of the FSS which formed a protective thin film layer that prevents hydrogen ion (H^+) ion release.
- The adsorbed protective film's SEM morphology on the FSS surface verified elevated performance of the green extract's inhibitive impact.
- The findings achieved using various analysis of corrosion (gravimetric and potentiodynamic polarization) are inappropriate contracts.

Acknowledgement

The authors are grateful for the technical assistance received from the staff of the Chemical, Metallurgical and Materials Engineering Department, Tshwane Technology University, South African. We are also thankful for the employees of Zaria, the National Chemical Technology Research Institute..

REFERENCES

- Al-Moubaraki, A.H et al; (2015) Corrosion of C-steel in the Red Sea: effect of immersion time and inhibitor concentration. *Int J ElectrochemSci* 10: 4252–4278
- Al-Otaibi, M. S et al; (2014) Corrosion inhibitory action of some plant extracts on the corrosion of mild steel in acidic media. *Arab J Chem* 7:340–346.
- Al-Fakih, A.M et al; (2015) Turmeric and ginger as green inhibitors of mild steel corrosion in acidic medium. *J Mater Environ Sci* 6:1480–1487
- Ahamed, H.A.U, Uddin MH, Mannan MA, Barua S, Hoque MA (2014) Studies on the isolation, physico-chemical characterization and microbial activities of melon (*Cucumis melon*) seed oil. *Int J Innov. Sci. Res.* 11:105–111

- Anupama, KK, Ramya K, Joseph A (2016) Electrochemical and computational aspects of surface interaction and corrosion inhibition of mild steel in hydrochloric acid by *Phyllanthusamarus* leaf extract (PAE). *J MolLiq* 216:146–155. <https://doi.org/10.1016/j.molliq.2016.01.019>.
- Adindu, C.B, Oguzie E.E (2017) Investigating the extract constituents and corrosion inhibiting ability of *Sidaacuta* leaves. *World News Nat Sci* 13:63–81.
- Borgioli, F, Galvanetto E, Bacci T. (2016): Low temperature nitriding of AISI 300 and 200 series austenitic stainless steels. *Vacuum*. Vol.127:51–60.
- Doner, A. et al; (2012) Experimental and theoretical studies of thiazoles as corrosion inhibitors for mild steel in sulphuric acid solution. *CorrosSci* 53:2902–2913
- Deyab, M.A (2015) Egyptian licorice extract as a green corrosion inhibitor for copper in hydrochloric acid solution. *J IndEngChem* 22:384–389.
- Emran, K.M et al; (2015) Corrosion and corrosion inhibition of cast Iron in hydrochloric acid (HCl) solution by cantaloupe (*Cucumis melo*) as green inhibitor. *Afr J Pure Appl Chem* 9:39–49.
- Fattah-alhosseini, A, Vafaeian S. (2016): Influence of grain refinement on the electrochemical behavior of AISI 430 ferritic stainless steel in an alkaline solution. *Applied Surface Science*. Vol.36:921–928
- Granese, S.L, Rosales, B.M. Ovideo, C, Zeriba J.O. (1992) The inhibition action of heterocyclic nitrogen organic compounds on Fe and steel in HCl media, *Corros.Sci.*, 33, 1439–1453.
- Hong, S et al; (2013) Investigation of the inhibition effect of trithiocyanuric acid on corrosion of copper in 3.0 wt% NaCl. *CorrosSci* 66:308–314.
- Ituen, E.B, Essien EA, Udo UE, Oluwaseyi OR (2014) Experimental and theoretical study of corrosion inhibition effect of *Cucumeropsis mannii* N. seed oil metallic soap of zinc on mild steel surface in sulphuric acid. *AdvApplSci Res* 5(3):26–53
- Khatak, H.S. Baldey, R. (2002) Corrosion of Austenitic Stainless Steels: Mechanism, Mitigation and Monitoring. ASM International. Narosa Publishing House. 1st ed.
- Kubmarawa, D et al; (2007) Preliminary phytochemical and antimicrobial screening of 50 medicinal plants in Nigeria. *Afr J Biotechnol* 6:1690–1696.
- Khadraoui, A et al; (2014) Adsorption and inhibitive properties of *Rutachalepensis* L. oil as a green inhibitor of steel in 1M hydrochloric acid medium. *Int J Electrochem Sci.*, 9:3334–3348.
- Kadry, S. (2008) Corrosion analysis of stainless steel, *Eur. J. Scientific Res.*, 22, 508–516.
- Okamoto, G. (1973) Passive film of 18-8 stainless steel structure and its function, *Corros. Sci.*, 13, 471–489.
- Pereira S.A 2012. Inhibitory action of aqueous garlic peel extract on the corrosion of carbon steel in HCl solution. *CorrosSci* 65:360–366.
- Rubaye, AYI et al. 2015. Cheery sticks plant extract as a green corrosion inhibitor complemented with LC-EIS/MS spectroscopy. *Int J ElectrochemSci* 10:8200–8209.
- Qian, Z et al; (2017) The corrosion inhibition effect of triazinedithiol inhibitors for aluminum alloy in a 1M HCl Solution. *Metals* 44:1–16.
- Rocha, JC, Gomes JACP, Elia ED (2014) Aqueous extracts of mango and orange peel as green inhibitors for carbon steel in hydrochloric acid solution. *Mater Res* 17:1581–1587.
- Sedriks, A.J. (1979) Corrosion of Stainless Steel, Wiley-Interscience, New York.
- Sharma, P, Roy, H. (2014): Pitting corrosion failure of an AISI stainless steel pointer rod. *Engineering Failure Analysis*. 44:400–407.
- Szypowski, A.J.S (2002) Impedance study of imidazoline inhibitors against hydrogen sulphide corrosion of steel, *Corros. J.* 37, 141–146.
- Suleiman, I.Y, Sani AS (2017) Characterizations of plant extract by AAS and GC–MS as green inhibitor for mild steel in 1.0 M HCl. *Iran J Sci Technol Trans A.* <https://doi.org/10.1007/s40995-017-0384-9>.
- Suleiman, I.Y, Yaro SA, Abdulwahab M (2016) Inhibitive behaviour of acacia senegalensis on corrosion resistance of mild steel in acidic environment. *Asian J Chem* 28:242–248.
- Suleiman, I.Y, Abdulwahab, M, Awe, F.E (2016) Green corrosion inhibition of *Acacia tortilis* extract on mild steel-sulphuric acid environment. *J Adv Electrochem* 2:50–55.
- Suleiman, I. Y., Mohammed A. T., Sirajo M. Z, Ochu S.R 2018. Synergistic Effect and Statistical Model of *Terminalia avicennoides* Anti-corrosion Inhibitor of Steel Pipelines in Acidic Environment. *Journal of Bio- and Tribo-Corrosion* (2018) 4:48 <https://doi.org/10.1007/s40735-018-0164-x>.
- Umoren, S.A, Eduok UM. 2016. Application of carbohydrate polymers as corrosion inhibitors for metal substrates in different media: a review. *Carbohydr Poly* 140:314–341.
- Verma, C, Quraishi M.A, Ebenso, E.E, Obot IB, El Assry A 2016. 3-Amino alkylated indoles as corrosion inhibitors for mild steel in 1 M HCl: Experimental and theoretical studies. *J MolLiq* 219:647–660. <https://doi.org/10.1016/j.molliq.2016.04.024>.
- Xhanari K, Finsgar M. 2016. Organic corrosion inhibitors for aluminium and its alloys in acid solutions: a review. *RSC Adv* 6:62833–62857
- Zhang X, Fan L, Xu Y, Li J, Xiao X, Jiang L. 2015. Effect of aluminium on microstructure, mechanical properties and pitting corrosion resistance of ultra-pure 429 ferritic stainless steels. *Materials & Design (1980-2015)*. vol.65:682–689.
